

RESEARCH ARTICLE

Descriptor analysis of estrogen receptor β -selective ligands using 2-phenylquinoline, tetrahydrofluorenone and 3-hydroxy 6H-benzo[c]chromen-6-one scaffolds

Balaji¹, Ramanathan Muthiah¹, Sabarinath², Ramamurthy², and Chandrasekharan¹

¹Department of Pharmacology, PSG College of Pharmacy, Coimbatore, India and ²Department of Biotechnology, PSG College of Technology, Coimbatore, India

Abstract

Estrogen receptor beta (ER β) selective ligands have attracted much attention recently in the design of anti-cancer drugs that are devoid of the common side effects of estrogen. Structural studies of estrogen receptor alpha (ER α) and β revealed that there were considerable differences in their ligand-binding cavity and in their volume. Hence, the present study has hypothesized that size and shape descriptors can influence the affinity/selectivity of the ligands towards ER β . To prove the same, quantitative structure-activity relationship (QSAR) analyses were carried out using multiple regression analysis on 2-phenylquinoline, tetrahydrofluorenone and 3-hydroxy-6H-benzo[c]chromen-6-one series. Results indicate that increased lipophilicity, decrease in ellipsoidal volume and width of substituents, presence of halogen atoms was essential for the ligands to have high affinity/selectivity towards ER β . QSAR models obtained were both internally and externally validated. The study delineates that the size and shape descriptors are best modulators of ER β affinity/selectivity. Docking studies were performed to support our QSAR results.

Keywords: Estrogen, ER α and β receptors, anti-cancer, phenylquinoline, tetrahydrofluorenone, 3-hydroxy-6H-benzo[c]chromen-6-one

Introduction

The biological effects of estrogens are mediated through its interaction with estrogen receptors (ERs) two forms of which are known as estrogen receptor alpha (ER α) and estrogen receptor beta (ER β)¹. ER β , as a molecularly distinct receptor, was identified and cloned from rat prostate and ovarian cells², closely followed by cloning of the human and mouse homologues³⁻⁵. ER α has 595 amino acids, whereas ER β is 485 amino acids long. The ER isoforms share 95% and 58% amino acid sequence identity in their DNA binding and ligand-binding domains (LBD), respectively⁶. The realization that there are two ERs with different tissue distribution raises the possibility of developing subtype selective ligands that can be used in a multitude of clinical states including hormone influenced cancer⁷. Further ER β agonists have minimal risk of adverse effects thus differing from

selective ER modulators that increase the risk of endometrial cancer⁸.

Currently, no selective ER β agonist is available in the market. Hence, to provide a rationale in the design of new anti-cancer agents, quantitative structure-activity relationship (QSAR) studies were employed. Several QSAR models on estrogens were derived in which most of them reported the estimation of different chemical class endocrine disruption potential⁹⁻¹¹ otherwise focused on the classification of ER agonist vs. non-agonist regardless of ER isoforms¹². Few authors^{13,14} had studied the structural features influencing the binding affinity to ER β using environmental estrogenic chemicals and phytoestrogens as data set (48 compounds as training set and 12 compounds as test set) in which they concluded that quantum chemical and electrostatic descriptors mainly

Address for Correspondence: Dr. Ramanathan Muthiah, M.Pharm, Ph.D, Department of Pharmacology, PSG College of Pharmacy, Peelamedu, Coimbatore, 641004 India. Tel.: +91 422 4345840. Fax: +91 422 2594400. E-mail: muthiah.in@gmail.com

(Received 06 March 2010; revised 19 February 2011; accepted 19 February 2011)

influenced the ER β selectivity. However, they concluded that their results on the external test set are not satisfactory in both receptor independent and dependent-based approach^{13,14}. Therefore, we intended to identify the features that will influence the ER β potency and selectivity. ER α and β isoforms differ in their ligand-binding pocket in two critical amino acids: Leu 384 and Met 421 in ER α , whereas the corresponding residues in ER β are Met 336 and Ile 373. In addition, ER β ligand-binding cavity is smaller (390Å³) compared to that of ER α (490Å³)¹⁵. These differences in binding site and volume between ER α and β LBD can be capitalized to design ER β selective ligands. To prove the same rationale, QSAR studies were employed on selective ER β series.

Materials and methods

Data set and software

The data used for our analyses were from the reported series of 2-phenylquinolines (21 compounds)¹⁶, tetrahydrofluorenones (31 compounds)¹⁷, and 3-hydroxy 6H-benzo[c]chromen-6-ones (28 compounds)¹⁸ since the series displayed a broad range of reactivity towards ERs (Table 1, 2 and 3). The same data set of Boriani et al.¹³ and Spreafico et al.¹⁴ was not taken because most of the ligands in their data set are non-selective or ER α selective. The structures of the ligands taken in the present study were constructed in DS Viewer Pro 6.0 (Accelrys Software Inc, 2005). Energy level of the constructed structures and

charges were optimized, and QSAR studies were carried out using a commercial package TSAR 3D, version 3.3 (Oxford Molecular Limited, 2000). Binding affinity for ER β (IC₅₀) and ER β selectivity (ER α IC₅₀/ER β IC₅₀ ratio) were considered as the biological activity of ligand-receptor interaction and were converted into the logarithmic scale. For the three series of compounds taken in the present study, a cluster analysis was carried out with TSAR using the complete linkage clustering method (Euclidean distances) with no data standardization for the whole data set comprising of descriptors and activity^{19,20}. Based on the clusters, the data set was divided into training and test sets so that all clusters are properly represented in both training and test sets in the ratio 3:1²⁰.

Descriptors selection

TSAR includes many structural property parameters like mass, surface area, volume, moments of inertia, molar refractivity, lipophilicity, verloop parameters, dipole, topological indices, connectivity indices, electrotopological state indices (E-state indices), Kier and Hall indices, number of atoms, rings, hydrogen bond acceptors and donors and Vamp electrostatic parameters. From the earlier crystallographic report¹⁵, we hypothesized that size and shape of the ligands mainly influence the ER β potency and selectivity. To prove the hypothesis, in the current study size and shape parameters like molecular weight, verloop, volume, kappa indices and number of atoms were included. Since atom-type E-state indices

Table 1. Structural features, observed and predicted ER β IC₅₀ values and ER α / β fold selectivity for 2-phenylquinoline scaffold.

S. No	R ¹	R ²	R ³	R ⁴	ER β IC ₅₀ (nM)		ER α / β	
					Observed	Predicted	Observed	Predicted
1	H	H	H	H	2.232	2.220	1.000	1.017*
2	H	H	Cl	H	1.477	1.765*	1.322	#
3	H	H	Br	H	1.944	2.051	1.113	1.370
4	H	H	H	Cl	0.662	1.129*	1.662	1.712
5	F	H	H	Cl	0.724	0.743	1.662	1.387*
6	H	H	H	Br	0.633	0.888*	1.698	1.630
7	F	H	H	Br	0.531	0.503	1.919	1.634
8	F	F	H	Br	1.556	1.364	1.342	1.325
9	H	H	H	CH=CH ₂	1.778	1.650*	0.903	0.697*
10	F	H	H	CH=CH ₂	1.643	1.915	0.954	1.105
11	H	H	H	C ₂ H ₅	1.716	#	1.079	1.192
12	F	H	H	C ₂ H ₅	1.897	1.632	1.342	0.836*
13	H	H	H	C \equiv CH	1.875	2.060*	1.301	1.011
14	F	H	H	C \equiv CH	1.431	1.938	1.681	0.957*
15	F	F	H	C \equiv CH	2.875	2.266	0.778	0.795
16	H	H	H	CN	1.447	1.526	1.204	#
17	F	H	H	CN	1.361	1.579*	1.662	1.491
18	H	H	H	COCH ₃	2.344	2.365	1.146	0.994*
19	F	H	H	COCH ₃	1.968	2.067	1.556	1.338
20	F	H	H	C ₆ H ₅	2.324	#	1.278	1.421
21	H	H	H	OCH ₃	3.075	2.260*	0.778	0.403*

*Compounds used in the test set.

#Outlier.

Table 2. Structural features, observed and predicted ER β IC₅₀ values and ER α / β fold selectivity for tetrahydrofluorenone scaffold.

S. No	<i>R</i> ¹	<i>R</i> ²	ER β IC ₅₀ (nM)		ER α / β	
			Observed	Predicted	Observed	Predicted
1	H	H	3.186	3.164	0.845	0.884
2	CH ₃	H	2.971	2.998	0.698	0.652*
3	C ₂ H ₅	H	2.572	2.846	1.431	#
4	CH ₃ CH ₂ CH ₂	H	2.338	2.694	1.079	1.195
5	CH ₃ CH ₂ CH ₂ CH ₂	H	2.274	2.544*	1.531	#
6	CH ₃ CH ₂ CH ₂ CH ₂ CH ₂	H	2.975	2.390	0.602	0.557
7	C ₆ H ₅ CH ₂	H	3.625	2.381*	0.301	0.625*
8	CH ₃	CH ₃	1.799	1.520*	1.278	1.477
9	C ₂ H ₅	CH ₃	1.447	1.366	1.633	1.416
10	CH ₃ CH ₂ CH ₂	CH ₃	1.041	1.237	1.414	1.417*
11	Iso-propyl	CH ₃	2.089	#	1.079	0.641*
12	CH ₃ CH ₂ CH ₂ CH ₂	CH ₃	1.204	1.063	1.591	1.417
13	Iso-butyl	CH ₃	1.301	1.099	1.000	#
14	C ₆ H ₅	CH ₃	1.176	1.076*	1.505	1.485
15	CH ₃	Br	1.127	0.877	1.819	1.785
16	C ₂ H ₅	Br	0.653	0.725	1.851	1.723
17	CH ₃ CH ₂ CH ₂	Br	0.643	0.576*	1.255	1.724*
18	CH ₃ CH ₂ CH ₂ CH ₂	Br	0.255	0.421	1.880	1.738
19	CH ₃ CH ₂ CH ₂ CH ₂	Et	1.113	0.521*	1.301	1.419*
20	CH ₃ CH ₂ CH ₂ CH ₂	Pr	0.176	0.369	1.301	1.418
21	CH ₃ CH ₂ CH ₂ CH ₂	Bu	1.176	0.294*	1.255	1.383
22	CH ₃ CH ₂ CH ₂ CH ₂	2-furyl	0.491	1.024	1.799	1.352*
23	CH ₃ CH ₂ CH ₂ CH ₂	2-thienyl	0.204	0.179	1.653	1.494
24	CH ₃ CH ₂ CH ₂ CH ₂	Phenyl	0.079	0.548*	1.531	1.364
25	CH ₃ CH ₂ CH ₂ CH ₂	CN	1.579	1.397	1.633	1.419*
26	CH ₃ CH ₂ CH ₂ CH ₂	CF ₃	0.176	-1.822*	1.929	1.965
27	CH ₃ CH ₂ CH ₂ CH ₂	Cl	0.724	0.722	1.342	1.544
28	CH ₃ CH ₂ CH ₂ CH ₂	I	0.113	-0.007*	1.977	1.884*
29	C ₆ H ₅	Br	0.397	0.410	1.653	1.788
30	C ₆ H ₅	2-furyl	1.204	0.977	1.380	1.487
31	C ₆ H ₅	CN	1.505	1.386	1.477	1.468*

*Compounds used in the test set.

#Outlier.

code mainly about size, cyclicality, branching and the number of quaternary atoms, which are found out by the rotation of high dimension space in different directions, it has also been included in the study²¹. Crystallographic and docking studies revealed that ER β selective ligands form hydrogen-bonding interactions with Glu 305, Arg 346 and His 475 of ER β ²². Hence, the number of hydrogen bond donors and acceptors were taken into account. The descriptors used in the present study are tabulated in Table 4.

Model construction and validation

Multi-parametric regression analyses between physico-chemical descriptors and biological activities were carried out to identify the favourable and adverse parameters for ER β potency and selectivity. Combinations of predictor variables were selected for further analyses based on low

interrelationship between them ($|R| < 0.6$)²³. Correlation matrices between the descriptors were given in the supplementary information. The robustness of the models and their internal predictive ability were evaluated by q^2 based on leave-more-out cross-validation (LMO_{cv}). The LMO_{cv} procedure consists of removing three examples from the training set and constructing the model only on the basis of the remaining training data and then testing on the removed examples. In this fashion, all of the training data examples were tested, and q^2 was calculated. Compounds were considered as outliers on the basis of their deviation between observed and predicted activities from the model (observed activity–predicted activity > 2 S.D., where S.D. is the standard deviation)²⁴. In order to find out any chance correlations associated with the QSAR models recognized in multiple linear regression analysis, each cross-validated model has been put to a

randomization test. Randomization was performed in Strike, Schrödinger²⁵ which is a chemically aware statistical tool. In this test, the dependent-variable (ER β affinity and selectivity) was randomly shuffled and a new QSAR model was developed for each respective series using the unchanged independent variable matrix. This process was repeated for several cycles. It was expected that the resulting QSAR models should have low randomized R^2 and high S.D. values²³. This is a widely used technique to ensure the robustness of a particular QSAR model. Over fitting, due to the excessive number of parameters (which increases the R and S.D values also), can be detected by the examination of Q value. Q is the quality factor ($Q=r/S.D.$)²³. In addition the developed model should be robust enough to be capable of making accurate and reliable predictions of biological activities of new compounds²⁶. Hence, in the present study, external validation was also carried out which consists of making predictions for an independent set of compounds not used in the model training. The correlation equations,

which returned the highest correlation coefficient (R^2), Fischer's value (F) and q^2 LMO_{cv} and lowest standard error of the regression model(s) were finally retained for further discussion. Predictability of the generated QSAR equations was externally validated using the test set and is denoted as R^2_{pred} .

Docking studies with the target ER β

Ligand preparation

The most active compound and least active compound of each series were identified and prepared for docking using LigPrep²⁷. LigPrep is a utility of Schrödinger software that generates 3D structures from 2D representation. LigPrep also assigns an appropriate bond order with correct chiralities for each successfully processed input structure and produce a number of structures from each input structure with various ionization states, tautomers, stereoisomers and ring conformations. Subsequently, the structures were optimized by means of OPLS-2005 using a default setting in the LigPrep.

Table 3. Structural features, observed and predicted values for ER β IC₅₀ values and ER α/β fold selectivity for 3-hydroxy- 6H-benzo[c] chromen-6-one scaffold.

S. No.	R^1	R^2	R^3	R^4	R^5	ER β IC ₅₀ (nM)		ER α/β	
						Observed	Predicted	Observed	Predicted
1	CH ₃	CH ₃	H	H	H	1.968	2.326*	2.029	1.560
2	CH ₃	H	OCH ₃	H	H	2.488	2.634	1.505	0.966*
3	CH ₃	H	Br	H	H	2.107	2.826	1.892	1.594
4	CH ₃	H	H	H	H	3.161	2.363*	0.845	0.965
5	CH ₃	H	CH=CH ₂	H	H	2.491	2.047	1.176	1.556*
6	H	H	CH ₃	H	CH ₃	1.954	2.106	0.812	#
7	C ₂ H ₅	H	Br	H	H	3.369	#	0.361	0.553
8	CH ₃	H	H	H	CH ₃	2.513	2.137	1.477	1.601*
9	CH ₃	H	H	H	CH=CH ₂	2.318	2.044*	1.681	1.608
10	CH ₃	H	H	H	Propenyl	2.064	1.424	1.414	#
11	CH ₃	CH ₃	OCH ₃	H	H	2.068	2.164*	1.929	1.004*
12	CH ₃	CH ₃	NH ₂	H	H	2.445	2.591	1.707	1.573
13	CH ₃	CH ₃	NHSO ₂ CH ₃	H	H	2.636	2.696*	0.991	1.621
14	CH ₃	Br	H	Br	H	1.380	1.494	1.397	1.553
15	CH ₃	CH ₃	H	H	CH ₃	1.903	1.761	1.579	1.837
16	CH ₃	CH ₃	NHCHO	H	H	2.980	2.533	1.000	1.025*
17	CH ₃	H	Br	CH ₃	H	2.332	2.204	1.505	1.549
18	CH ₃	H	OCH ₃	Br	H	1.886	1.874	2.110	#
19	CH ₃	H	Br	Butenyl	H	1.414	1.234	1.623	1.744*
20	CH ₃	H	CH ₃	H	CH ₃	1.301	1.550*	2.264	2.367
21	CH ₃	H	CH ₃	H	Br	1.643	1.653	1.851	1.427
22	CH ₃	H	CH ₃	H	H ₂ C=CH-CH ₂	1.544	1.159*	2.454	2.395
23	CH ₃	H	CH ₃	H	CH=CH ₂	1.000	1.405	3.000	2.716*
24	CH ₃	H	OCH ₃	H	CH ₃ CH ₂	1.838	1.691*	2.152	1.916
25	CH ₃	H	OCH ₃	H	CH=CH ₂	1.724	1.923	2.274	2.458
26	CH ₃	H	CH ₃	Br	CH ₃	1.755	1.444*	2.243	2.133*
27	CH ₃	H	CH ₃	OCH ₃	CH ₃	1.204	1.053	2.411	2.411
28	CH ₃	Br	CH ₃	OCH ₃	CH ₃	0.060	0.680	2.176	2.185*

*Compounds used in the test set.

#Outlier.

Table 4. Molecular descriptors selected for the study.

Descriptors	Class of descriptor
Molecular weight	Structural
Number of atoms	Structural
Number of halogen atoms	Structural
Number of heteroatoms	Structural
Number of hydrogen bond donors	Structural
Number of hydrogen bond acceptors	Structural
Ellipsoidal volume	Spatial
Verloop L, B1-B5	Steric
Kappa indices (α 1-3)	Shape
Lipophilicity	Thermodynamic
Electrotopological state indices	Electronic

Protein preparation

The X-ray crystal protein structure of ER β in complex with compound genistein (PDB ID: 1QKM, resolution 1.8Å) obtained from the RCSB Protein Data Bank (PDB) was used in this study²⁸. Many recent computational studies on ER β used the crystal structure 1QKM to predict the binding modes of ER β compounds^{18,22}. Protein structure was prepared using the Maestro software package²⁹ and aligned using the protein structure alignment module in Prime³⁰. Bond orders and formal charges were added for heterogroups, and hydrogens were added to all atoms in the system. Protein was inspected visually for accuracy in the χ^2 dihedral angle of Asn and His residues and the χ^3 angle of Gln, and rotated by 180° when needed to maximize hydrogen bonding. The proper His tautomer was also manually selected to maximize hydrogen bonding. All Asp, Glu, Arg and Lys residues were left in their charged state. Water molecules of crystallization were removed from the complex except in the active site. A brief relaxation was performed on structure using the Protein Preparation module in Maestro with the “Refinement Only” option. This is a two-part procedure that consists of optimizing hydroxyl and thiol torsions in the first stage followed by an all-atom constrained minimization carried out with the Impact Refinement module (Impref) using the OPLS-2005 force field to alleviate steric clashes that may exist in the original PDB structures. The minimization was terminated when the the root mean square deviation (RMSD) reached a maximum cutoff of 0.30 Å.

Grid generation and ligand docking

Grids were defined by centring them around the ligand in the crystal structure using the default box size setting in Glide: scaling of van der Waals radii of protein atoms partial atomic charge of less than 0.25 by 1.0. Hydrogen bond constraints were not applied. Flips of 5- and 6-member rings were allowed, and non-planar conformation of amide bonds was penalized. van der Waals radii of ligand atoms with partial atomic charge less than 0.15 was scaled by 0.8. The prepared ligands were docked against the ER β receptor. All docking calculations were performed using the “Extra precision” (XP) mode of Glide program³¹.

Glide uses a hierarchical series of filters to search for possible locations of the ligand in the active-site

region of the receptor. The initial filters test the spatial fit of the ligand to the defined active site, and examine the complementarity of ligand–receptor interactions using a grid-based method. Poses that pass these initial screens enter the final stage of the algorithm, which involves evaluation and minimization of a grid approximation to the OPLS-AA nonbonded ligand–receptor interaction energy. Final scoring is then carried out on the energy-minimized poses. The minimized poses are rescored using Schrödinger’s proprietary GlideScore (GScore) scoring function. GScore is a modified version of ChemScore, but includes a steric-clash term and adds buried polar terms devised by Schrödinger to penalize electrostatic mismatches.

$$\text{GScore} = a \times \text{vdW} + b \times \text{Coul} + \text{Lipo} + \text{Hbond} + \text{Metal} + \text{BuryP} + \text{RotB} + \text{Site}$$

where vdW—Van der Waal energy, Coul—Coulomb energy, Lipo—Lipophilic contact term, Hbond—Hydrogen-bonding term, Metal—Metal-binding term, BuryP—Penalty for buried polar groups, RotB—Penalty for freezing rotatable bonds, Site—Polar interactions at the active site; and the coefficients of vdW and Coul are: $a=0.065$, $b=0.130$. All docking computations were carried out with the Linux OS (Red Hat Enterprise WS 5.0).

Results and discussion

Many structurally diverse compounds have been noted to engage ERs and influence cellular response through them. ER LBD recognizes a wide variety of structurally distinct compounds that act as either receptor agonists, antagonists or have mixed character. In the present study, three structurally different compounds and their derivatives were analyzed for their molecular attributes such as size or shape parameters, lipophilicity and hydrogen-bonding potential. Molecular recognition of estrogenic compounds is achieved through a combination of specific hydrogen bonds with the receptor and hydrophobic interaction between residues that line the receptor cavity and the non-polar region of the ER ligands. Structural plasticity also allows ERs to shrink the cavities by as much as 15% to accommodate the smaller ligands better³². Thus, the ability of ER to bind a wide range of compounds stems from the flexibility in both the size and shape of the LBD. In the present study, we have considered size and shape indices of the ligands, in addition to their chemical characteristics important in determining ER β potency and selectivity. Further, earlier report indicates that the differing amino acid at position Met 421 (ER α) and the corresponding Ile 373 (ER β) would be an important differentiator in determining the specificity of ligand interaction than the other differing amino acid pair, viz Leu 384 (ER α) and Met 336 (ER β)³³. In ER α , Met 421 makes a repulsive interaction with the electronegative and the non-polarisable groups³³, and hence the electrotopological state (E-state index) was considered to be one of the differentiating descriptors to determine ligand selectivity. Before docking study, the

original crystal structure of ER β -genistein complex (PDB ID: 1QKM) was used to validate the Glide-XP docking protocol. This was carried out by removing the co-crystallized genistein ligand outside the active site and then docked back in to the active site. The RMSD was calculated for the best configuration in comparison to the co-crystallized genistein, and it was found to be 1.30 Å. The hydrogen bonding interactions between the genistein and ER β was found to be in accordance with the crystallographic data²⁸. Docking results of best active and least active compounds of the phenylquinoline, tetrahydrofluorenone and 3-hydroxy-6H-benzo[c]chromene-6-one series was taken to support our QSAR results.

Phenylquinoline

The chemical structure of 2-phenylquinoline is shown in Figure 1A. Parameters like molecular weight, number of hydrogen bond donors and acceptors, verloop parameters and E-state indices did not show any statistically significant effect on receptor activation and hence not reported here. The parameters showing significant

relationship with receptor interaction are shown in Table 5. A multi-parameter regression model for the ER β receptor binding and ER α to ER β selectivity is shown in Equation 1 and Equation 2 below.

$$\log [\text{IC50}]_{\beta} = -0.877 \times a - 0.636 \times b + 5.421 \quad (1)$$

where a = lipophilicity (whole molecule) and b = number of heteroatoms at R^4 .

$$\log ([\text{IC50}]_{\alpha} / [\text{IC50}]_{\beta}) = -0.001 \times a - 0.530 \times b + 1.981 \quad (2)$$

where a = ellipsoidal volume (whole molecule) and b = kappa 2 index of substituents at R^2 .

These equations predict the binding affinity (Figure 2A) and ER β selectivity (Figure 2B) using the indicated descriptors. The plot against the observed vs. predicted values depict a good fit, and the statistical parameters are significant which suggests the utility of the model (Table 6). The propensity for a ligand to bind with higher affinity to ER β is correlated with higher LogP (ER α binding affinity decreases with increase in lipophilicity). This is consistent with the ER β binding pocket where large lipophilic cavities are present. Hence it is not surprising that log P is a modulator for ER β affinity. Earlier reports also indicate that hydrophobic compounds exhibited better ER β potency³⁴ that is consistent with the present findings. Equation 1 suggests that incorporation of heteroatoms at R^4 of phenylquinolines will increase the ER β affinity. From Table 1, it can be inferred that a wide variety of functional groups including electronegative, electron-rich, aliphatic, aromatic, and polar

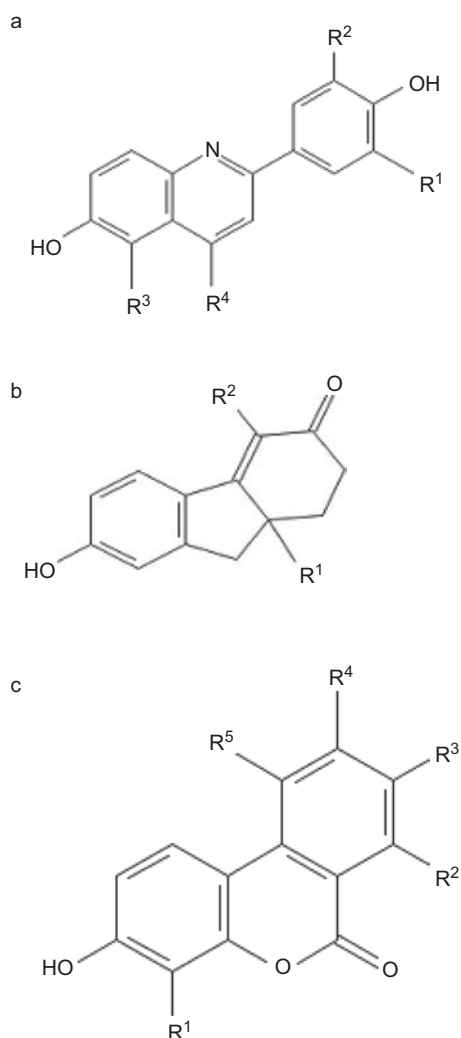


Figure 1. Skeletal structure of estrogenic compounds. The moieties derivatised in each compound is indicated and referred in the Tables 1, 2, and 3.

Table 5. Physicochemical descriptors that significantly influenced the 2-phenylquinoline derivatives binding at ER receptors.

S. No.	Log P	Number of heteroatoms at R^4	Ellipsoidal volume (whole molecule)	Kappa 2 index of substituents at R^2
1	3.650	0	963.503	0.0
2	4.168	0	883.183	0.0
3	3.842	0	1307.560	0.0
4	4.168	1	576.104	0.0
5	4.608	1	593.980	0.0
6	4.442	1	750.821	0.0
7	4.882	1	742.811	0.0
8	3.901	1	836.976	0.5
9	4.299	0	1284.100	0.0
10	3.998	0	1874.880	0.0
11	4.216	0	1689.270	0.0
12	4.321	0	1324.970	0.0
13	3.832	0	2075.810	0.0
14	3.971	0	1386.10	0.0
15	3.598	0	1971.28	0.5
16	3.715	1	986.599	0.0
17	3.655	1	1049.600	0.0
18	2.759	1	1287.69	0.0
19	3.098	1	1376.590	0.0
20	5.174	0	1199.310	0.0
21	2.879	1	1577.20	0.0

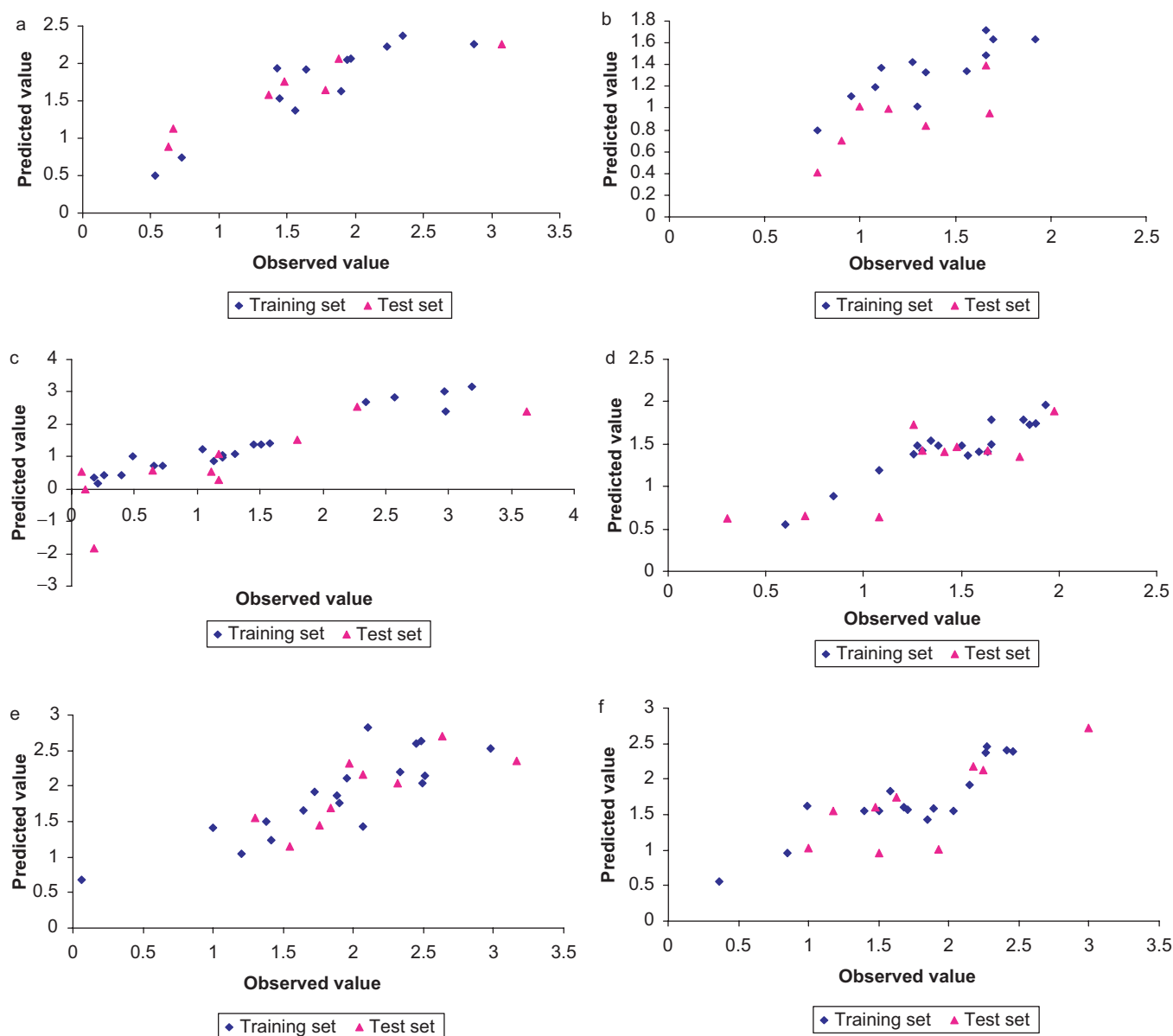


Figure 2. Plot of predicted vs. observed values of ER β binding affinity and fold selectivity of the ligands against ER receptors. (A), (C) and (E) represent the ER β binding affinity of phenylquinoline, tetrahydrofluorenone and 3-hydroxy 6H-benzo[c]chromen-6-one ligands respectively. (B), (D) and (F) represent the ER β fold selectivity of phenylquinoline, tetrahydrofluorenone and 3-hydroxy 6H-benzo[c]chromen-6-one ligands, respectively.

Table 6. QSAR statistics of the best multiple linear regression equations.

Data set	<i>n</i>	<i>R</i> ²	<i>R</i>	S.D.	<i>Q</i>	<i>q</i> ²	<i>F</i> value	RMSE		Randomized		
								Training set	Test set	<i>R</i> ²	S.D.	<i>R</i> ² _{pred}
2-phenylquinoline ER β IC ₅₀	12	0.822	0.906	0.305	2.970	0.720	20.849	0.264	0.395	0.131	0.785	0.853
2-phenylquinoline ER α/β	12	0.724	0.850	0.217	3.917	0.579	19.048	0.173	0.226	0.192	0.621	0.548
Tetrahydrofluorenone ER β IC ₅₀	20	0.934	0.966	0.270	3.577	0.758	75.970	0.245	0.707	0.174	0.537	0.652
Tetrahydrofluorenone ER α/β	18	0.850	0.921	0.147	6.265	0.717	42.700	0.134	0.278	0.101	0.724	0.667
3-hydroxy 6H-benzo[c]chromen-6-one ER β IC ₅₀	18	0.723	0.850	0.385	2.207	0.556	19.671	0.351	0.338	0.142	0.697	0.612
3-hydroxy 6H-benzo[c]chromen-6-one ER α/β	16	0.780	0.883	0.310	2.848	0.602	14.194	0.268	0.373	0.157	0.954	0.625

substituents were introduced at R^4 of phenylquinolines. Among which, compounds that had electronegative substitutions showed increased affinity towards ER β (Table 1). According to Vu et al.¹⁶, Met 421 of ER α and Ile 373 of ER β interacts with the residue at R^4 of phenylquinolines. Although the relative contribution of dispersion, electrostatics and exchange repulsion is unclear, it is possible that the electronegativity of the halogens and the methionine sulphur makes an unfavourable electrostatic contribution to the total interaction with ER α thereby increasing the affinity towards ER β . The repulsion with Met421 of ER α by halides created at this site could permit better moulding with ER β receptor. In the present study, docking of most active compound 7 in the 2-phenylquinoline series to the binding pocket of the ER β places the bromo group at R^4 in close proximity to the ER β Ile373 residue (Figure 3A) and showed more GScore than the inactive compound 21 in the series. This is in concordance with the earlier report that chemically hard functional group containing electronegative atoms are more attractive synthetic target than others with regard to improved ER β binding³³. Interestingly, compound 21 containing methoxy group at R^4 substitution exhibited a great loss of affinity, presumably due to the unfavourable basicity of the quinoline core induced by the electron-rich methoxy group¹⁶.

In the present study, Equation 2 indicates that decrease in ellipsoidal volume increases the fold selectivity towards ER β . From Table 5, it can be seen that compounds having aliphatic groups such as ethyl, vinyl, alkynyl, and electron-withdrawing cyano group displayed higher ellipsoidal volume and showed only minimal selectivity. Compounds substituted with halides at R^4 position displayed low ellipsoidal volume and displayed higher selectivity which is in accordance with the present study results (Equation 2). This may be because the internal volume of the LBD of ER β is significantly smaller (~20%) than in ER α and hence it may have implications for the selectivity of ligands. Equation 2 also indicates that kappa 2 indices of the substituents at R^2 should be less to have increased selectivity in phenylquinolines. The kappa index is the molecular shape index based on the assumption that the shape of a molecule is a function of the number of atoms and their bonding relationship. Kappa 2 index indicates the degree of linearity of bonding patterns³⁵. From Table 1, it can be inferred that substitution at R^2 decreases the selectivity of the compounds towards ER β (compare compound 7 vs. 8, 14 vs. 15) which is in accordance with Equation 2.

Tetrahydrofluorenone

The structure of tetrahydrofluorenone is shown in Figure 1B. Among the various descriptors analyzed, the molecular weight, molecular surface area, number of hydrogen bond donors/acceptors, ellipsoidal volume, kappa indices and E-state indices were not significantly correlated with ER β affinity/selectivity and hence not discussed further. The descriptors showing significant

influence on ER β affinity/selectivity are shown in Table 7. The multi-parameter regression analysis is for ER β receptor binding and ER β to ER α selectivity is described as in Equation 3 and Equation 4 below.

$$\log [IC50]_{\beta} = -1.953 \times a - 0.383 \times b - 0.295 \times c + 5.752 \quad (3)$$

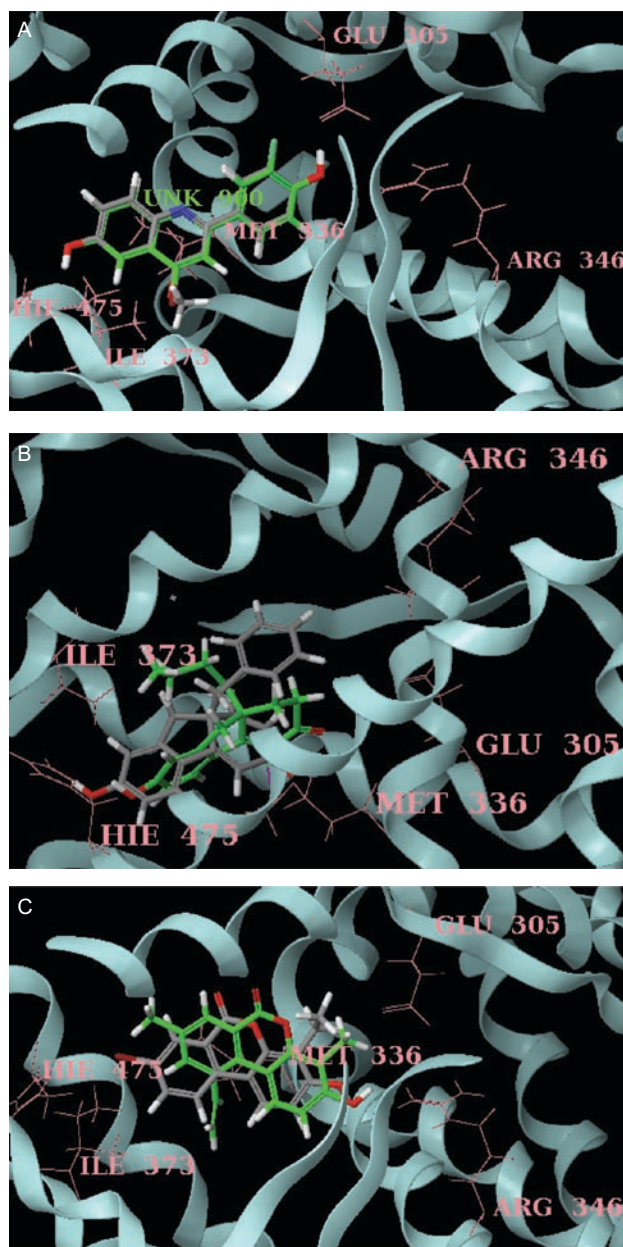


Figure 3. (A) Docked pose of most active compound 7 (green) and least active compound 21 (grey) in the phenylquinoline series with ER β . Only key residues (pink), of the ER β binding site are shown for simplicity. (B) Docked pose of most active compound 28 (green) and least active compound 7 (grey) in the tetrahydrofluorenone series with ER β . Only key residues (pink), of the ER β binding site are shown for simplicity. (C) Docked pose of most active compound 23 (green) and least active compound 7 (grey) in the tetrahydrofluorenone series with ER β . Only key residues (pink), of the ER β binding site are shown for simplicity.

where a =verloop B2 of substituents at R^2 b =lipophilicity (whole molecule) and c =number of halogen atoms at substituent R^2 .

$$\log ([IC50]_{\alpha}/[IC50]_{\beta}) = 1.223 \times a - 0.291 \times b - 0.047 \quad (4)$$

where a =verloop B1 of substituents at R^2 and b =verloop B2 of substituents at R^1 .

The observed experimental and the values predicted from Equations 3 and 4 are plotted in Figure 2C and 2D. Statistical parameters of Equations 3 and 4 were significant which indicate the robustness of the model (Table 6). Equation 3 indicates that increase in the width (verloop B2) of R^2 substituents will increase the ER β affinity of the ligands. From Table 2, it can be observed that introduction of methyl group at R^2 resulted in increase in ER β binding (compare compound 2 vs. 8). Further increase in width using substituents like heteroaryl or phenyl groups at R^2 increased the binding affinity (Table 2) which is in accord with the present study results (Equation 3). Like phenylquinolines, in tetrahydrofluorenone series also an increase in affinity for ER β was observed when the lipophilicity of the ligands increased. Equation 3 also reveals that presence of halogen atoms at R^2 increases the affinity of the compounds. From the docking studies of the most

active compound 28 in the tetrahydrofluorenone series, it was observed that the functional groups at R^2 interacted with Met 336 of ER β through van der Waal's force. This observation suggests that presence of halides near Met 336 will enhance ER β ligand interaction leading to increased affinity. This affinity enhancement for ER β can be attributed to a favourable overall hydrophobic effect due to the substituent (halogen) itself and additional van der Waals interactions between the halogen and surrounding residues. From Table 2, it can be inferred that halogenated analogues at R^2 showed more affinity towards ER β in contrast to heteroaryl and phenyl analogues.

Equation 4 indicates that increase in the width (verloop B1) of substituents at R^2 in tetrahydrofluorenones is favourable for increasing selectivity towards ER β . Verloop B1 is the width parameter and is defined as the smallest width of the substituent in any direction perpendicular to verloop length³⁶. As R^2 substituents are near to more flexible Met 336 of ER β , bulkier substituents can be well accommodated when compared to Leu 384 of ER α and display high selectivity. Equation 4 indicates that increase in width (verloop B2) of the substituents at R^1 will be detrimental to ER β selectivity. Verloop B2 is determined by measuring the width of the substituent

Table 7. Physicochemical descriptors that significantly influenced the tetrahydrofluorenone derivatives binding at ER receptors.

S. No.	Verloop B2 of R^2	Lipophilicity	Number of halogen atoms at R^2	Verloop B1 of R^2	Verloop B2 of R^1
1	1.000	1.653	0	1.000	1.000
2	1.000	2.086	0	1.000	1.800
3	1.000	2.483	0	1.000	1.889
4	1.000	2.879	0	1.000	1.835
5	1.000	3.275	0	1.000	1.898
6	1.000	3.672	0	1.000	2.120
7	1.000	3.700	0	1.000	1.892
8	1.702	2.364	0	1.650	1.696
9	1.703	2.761	0	1.650	1.902
10	1.691	3.157	0	1.650	1.903
11	1.701	3.091	0	1.650	2.659
12	1.702	3.553	0	1.650	1.899
13	1.697	3.487	0	1.650	1.899
14	1.691	3.581	0	1.650	1.666
15	1.900	2.262	1	1.900	1.689
16	1.900	2.658	1	1.900	1.900
17	1.900	3.055	1	1.900	1.897
18	1.900	3.451	1	1.900	1.849
19	1.903	3.949	0	1.650	1.895
20	1.902	4.346	0	1.650	1.896
21	1.864	4.742	0	1.650	2.018
22	1.690	3.719	0	1.650	2.124
23	2.055	4.062	0	1.713	1.903
24	1.728	4.770	0	1.650	2.080
25	1.650	2.951	0	1.650	1.896
26	2.646	3.969	3	2.168	2.195
27	1.800	3.177	1	1.800	2.093
28	2.030	3.917	1	2.030	1.892
29	1.900	3.479	1	1.900	1.677
30	1.708	3.747	0	1.650	1.661
31	1.650	2.979	0	1.650	1.725

in the direction opposite to the axis defined by B1. From Table 2, it can be inferred that selectivity of tetrahydrofluorenone increases when R^1 increases from methyl up to butyl, whereas when the substituents like pentyl, benzyl were introduced the selectivity of the compounds become detrimental towards ER β which is in accordance with Equation 4. Docking of most active compound 28 in the tetrahydrofluorenone series reveals that selectivity enhancing interaction is the putative favourable hydrophobic interaction between the n-butyl group at R^1 which protrudes orthogonally from the plane of the tricyclic core towards Ile373 in ER β as depicted in Figure 3B. We speculate that Ile373 in ER β can nicely accommodate the presence of the n-butyl moiety into space which is not available in ER α because the sidechain of the analogous Met 421 fills this space¹⁷. Docking of most inactive compound 7 in the tetrahydrofluorenone series reveals that substituent like benzyl in R^1 is not well accommodated near Ile373 of ER β and exhibited less GScore when compared with the active compound 7 of the same series.

3-hydroxy-6H-benzo[c]chromene-6-one

The structure of 3-hydroxy-6H-benzo[c]chromene-6-one is shown in Figure 1C. Analogues were obtained by derivatisation at five different positions. The physicochemical

properties of the analogues were determined as described in methods of which molecular weight, number of hydrogen bond donors/acceptors, lipophilicity, E-state indices were not found to be significantly influencing ER β receptor interaction or receptor preference, and hence not further discussed. The values for the other significant parameters are shown in Table 8. Multi-parameter regression analysis resulted in the numerical relationship of the descriptors to their reactivity with ER as given below.

$$\log [\text{IC50}]_{\beta} = -0.025 \times a + 0.569 \times b + 7.894 \quad (5)$$

where a = molecular surface area (whole molecule) and b = number of heteroatoms of substituents at R^3 .

$$\log ([\text{IC50}]_{\alpha} / [\text{IC50}]_{\beta}) = -5.027 \times a + 0.671 \times b + 0.466 \times c + 9.423 \quad (6)$$

$n = 16$; $R^2 = 0.780$; $s = 0.310$; $F = 14.194$; $\text{RMSE}_{\text{training set}} = 0.268$; $q^2 = 0.602$; $R^2_{\text{pred}} = 0.625$; $\text{RMSE}_{\text{test set}} = 0.373$

where a = verloop B2 of substituents at R^1 , b = verloop B3 of substituents at R^5 and c = κ Alpha 3 index of substituents at R^4 .

The values predicted by Equations 5 and 6 are plotted against experimentally observed values in Figure 2E

Table 8. Physicochemical descriptors that significantly influenced the 3-hydroxy 6H-benzo[c]chromen-6-one derivatives binding at ER receptors.

S. No.	Molecular surface area (whole molecule)	Number of heteroatoms at R^3	Verloop B2 of R^1	Verloop B3 of R^5	κ Alpha 3 index at R^4
1	218.480	0	1.697	1.000	0.000
2	227.157	1	1.815	1.000	0.000
3	219.649	1	1.690	1.000	0.000
4	218.036	0	1.815	1.000	0.000
5	227.817	0	1.698	1.000	0.000
6	225.502	0	1.000	1.902	0.000
7	245.908	1	1.897	1.000	0.000
8	224.297	0	1.808	1.895	0.000
9	235.489	0	1.805	1.880	0.000
10	252.072	0	1.716	1.925	0.000
11	248.048	1	1.808	1.000	0.000
12	228.816	1	1.694	1.000	0.000
13	279.919	4	1.685	1.000	0.000
14	249.354	0	1.698	1.000	0.000
15	238.977	0	1.810	2.056	0.000
16	253.295	2	1.804	1.000	0.000
17	243.910	1	1.699	1.000	0.000
18	256.760	1	1.703	1.000	0.000
19	281.690	1	1.816	1.000	3.351
20	239.776	0	1.688	2.034	0.000
21	243.152	0	1.804	1.600	0.000
22	267.061	0	1.695	2.228	0.000
23	252.842	0	1.683	1.868	0.000
24	266.523	1	1.789	2.220	0.000
25	254.838	1	1.689	2.279	0.000
26	259.945	0	1.703	1.897	0.000
27	266.543	0	1.810	1.966	1.649
28	281.078	0	1.791	1.903	1.649

and 2F, indicating a good fit between both sets of data and the statistical parameters indicate the utility of the QSAR model (Table 6). Equation 5 indicates that increase in molecular surface of chromenones will increase the affinity of the ligands towards ER β . This affinity enhancement may be attributed to the favourable van der Waals interactions of the chromenone ring and surrounding hydrophobic residues. In Table 3, it is noticeable that increasing the number of substituents (thereby molecular surface area) on the phenyl rings gives better ER β binding affinities. Compound 28 with five substituents on the aromatic rings has excellent binding affinity which is in accord with the results of Equation 5. Equation 5 indicates that increase in heteroatoms at R^3 decreases the ER β affinity remarkably. In the chromenone series, it can be observed that introduction of polar amino groups at R^3 decreases the ER β affinity (Table 3). Increasing the acidity of the amino group by substitution with electron-withdrawing groups (compounds 13 and 16) gave poorly active compounds because R^3 position is unable to sustain a group much larger than methyl (compounds 3,5,11) which is in accord with the QSAR results (Equation 5).

Equation 6 indicates that decrease in the width of substituents (verloop B2) at R^1 is required for increased ER β selectivity. Increase in verloop B2 (-CH₃ to -C₂H₅) in R^1 significantly reduced the selectivity of the molecule (compound 3 vs. 7, Table 3) towards ER β . This suggests that space availability was constrained to limit the size of the substituents at R^1 . Increase in width (verloop B3) of the substituents at R^5 increases the selectivity of the compounds towards ER β . Kappa index, another descriptor included in Equation 6, is a molecular shape index based on the assumption that the shape of a molecule is a function of the number of atoms and their bonding relationships. A group of modified indices, kappa alpha indices (κ Alpha) are calculated for each atom-type using the ratio of covalent radii of carbon (sp³) and the atom³⁵. Increase in κ Alpha 3 index of the substituent at R^4 increases the selectivity of the molecules towards ER β . In 3-hydroxy-6H-benzo[c]chromene-6-ones, compounds 19, 27, 28 displayed higher κ Alpha 3 indices and selectivity which is in accord with the QSAR Equation 6. Docking of the most active compound 23 in the 3-hydroxy-6H-benzo[c]chromene-6-one series revealed that the vinyl group in R^5 extends into the ER β Ile373 pocket and sits in a groove formed by Ile373, Ile376 and Phe377 (Figure 3C). The vinyl CH acts as a "hinge" that directs the ethylene moiety into this relatively narrow groove and forces it to be in close proximity to ER β Ile373 and hence leading to enhanced ER β selectivity. Similar interactions have been reported earlier with vinyl functional group in aryl diphenolic azoles⁶ and 7-substituted benzofuran and benzoxazoles³³ with ER β .

In the present study, QSAR analyses indicated that for the three different series of scaffolds, size and shape descriptors were able to explain the ER β potency and selectivity well. Further, the constructed QSAR models

in the present study were more reliable than the previously reported^{13,14} as they exhibited values of q^2 LMO_{cv} > 0.5; $R^2_{\text{pred}} > 0.6$ (except Equation 2) which represents the utility of the QSAR models²⁰. Low randomized R^2 and high S.D values were exhibited by the QSAR models in randomization test indicates that there is no chance correlation. High Q values (Table 6) of the obtained QSAR models indicate that there is no over fitting due to more number of descriptors³⁶. Root mean square error (RMSE) of all active compounds in the training test set for ER β in the previously reported QSAR model was 0.65, 1.22, respectively and the $R^2_{\text{pred}} = 0.42$ ¹³. In the present study, all the QSAR models showed less RMSE value which also represents the utility of the QSAR models.

In conclusion, among the descriptors studied, increased lipophilicity, decrease in ellipsoidal volume and width of substituents, presence of halogen atoms were essential for the ligands to have high affinity and selectivity towards ER β . The present study clearly delineates that the size and shape descriptors are the best modulators of ER β affinity and selectivity than the quantum chemical and electrostatic descriptors. Information presented here will not only enlarge the areas of their application, but it may also increase our understanding towards the mechanisms of chemical-biological interactions.

Declaration of interest

Authors declare no conflict of interest.

References

- Katzenellenbogen BS. Estrogen receptors: bioactivities and interactions with cell signaling pathways. *Biol Reprod* 1996;54:287-293.
- Kuiper GG, Enmark E, Peltö-Huikko M, Nilsson S, Gustafsson JA. Cloning of a novel receptor expressed in rat prostate and ovary. *Proc Natl Acad Sci USA* 1996;93:5925-5930.
- Mosselman S, Polman J, Dijkema R. ER beta: identification and characterization of a novel human estrogen receptor. *FEBS Lett* 1996;392:49-53.
- Enmark E, Peltö-Huikko M, Grandien K, Lagercrantz S, Lagercrantz J, Fried G et al. Human estrogen receptor beta-gene structure, chromosomal localization, and expression pattern. *J Clin Endocrinol Metab* 1997;82:4258-4265.
- Tremblay GB, Tremblay A, Copeland NG, Gilbert DJ, Jenkins NA, Labrie F et al. Cloning, chromosomal localization, and functional analysis of the murine estrogen receptor beta. *Mol Endocrinol* 1997;11:353-365.
- Malamas MS, Manas ES, McDevitt RE, Gunawan I, Xu ZB, Collini MD et al. Design and synthesis of aryl diphenolic azoles as potent and selective estrogen receptor-beta ligands. *J Med Chem* 2004;47:5021-5040.
- Imamov O, Shim GJ, Warner M, Gustafsson JA. Estrogen receptor beta in health and disease. *Biol Reprod* 2005;73:866-871.
- Koehler KE, Helguero LA, Haldosén LA, Warner M, Gustafsson JA. Reflections on the discovery and significance of estrogen receptor beta. *Endocr Rev* 2005;26:465-478.
- Vedani A, Smiesko M, Spreafico M, Peristera O, Dobler M. VirtualToxLab - in silico prediction of the toxic (endocrine-disrupting) potential of drugs, chemicals and natural products. Two years and 2,000 compounds of experience: a progress report. *Altex* 2009;26:167-176.

10. Cao Q, Garib V, Yu Q, Connell DW, Campitelli M. Quantitative structure-property relationships (QSPR) for steroidal compounds of environmental importance. *Chemosphere* 2009;76:453-459.
11. Roncaglioni A, Piclin N, Pintore M, Benfenati E. Binary classification models for endocrine disrupter effects mediated through the estrogen receptor. *SAR QSAR Environ Res* 2008;19:697-733.
12. Li H, Ung CY, Yap CW, Xue Y, Li ZR, Chen YZ. Prediction of estrogen receptor agonists and characterization of associated molecular descriptors by statistical learning methods. *J Mol Graph Model* 2006;25:313-323.
13. Boriani E, Spreafico M, Benfenati E, Novic M. Structural features of diverse ligands influencing binding affinities to estrogen alpha and estrogen beta receptors. Part I: Molecular descriptors calculated from minimal energy conformation of isolated ligands. *Mol Divers* 2007;11:153-169.
14. Spreafico M, Boriani E, Benfenati E, Novic M. Structural features of diverse ligands influencing binding affinities to estrogen alpha and estrogen beta receptors. Part II. Molecular descriptors calculated from conformation of the ligands in the complex resulting from previous docking study. *Mol Divers* 2007;11:171-181.
15. Hillisch A, Peters O, Kosemund D, Müller G, Walter A, Schneider B et al. Dissecting physiological roles of estrogen receptor alpha and beta with potent selective ligands from structure-based design. *Mol Endocrinol* 2004;18:1599-1609.
16. Vu AT, Cohn ST, Manas ES, Harris HA, Mewshaw RE. ERbeta ligands. Part 4: Synthesis and structure-activity relationships of a series of 2-phenylquinoline derivatives. *Bioorg Med Chem Lett* 2005;15:4520-4525.
17. Wilkening RR, Ratcliffe RW, Tynebor EC, Wildonger KJ, Fried AK, Hammond ML et al. The discovery of tetrahydrofluorenones as a new class of estrogen receptor beta-subtype selective ligands. *Bioorg Med Chem Lett* 2006;16:3489-3494.
18. Sun W, Cama LD, Birzin ET, Warriar S, Locco L, Mosley R et al. 6H-Benzo[c]chromen-6-one derivatives as selective ERbeta agonists. *Bioorg Med Chem Lett* 2006;16:1468-1472.
19. Trossini GH, Guido RV, Oliva G, Ferreira EI, Andricopulo AD. Quantitative structure-activity relationships for a series of inhibitors of cruzain from *Trypanosoma cruzi*: molecular modeling, CoMFA and CoMSIA studies. *J Mol Graph Model* 2009;28:3-11.
20. Leonard JT, Roy K. Exploring molecular shape analysis of styrylquinoline derivatives as HIV-1 integrase inhibitors. *Eur J Med Chem* 2008;43:81-92.
21. Hu QN, Liang YZ, Yin H, Peng XL, Fang KT. Structural interpretation of the topological index. 2. The molecular connectivity index, the kappa index, and the atom-type E-state index. *J Chem Inf Comput Sci* 2004;44:1193-1201.
22. Ullrich JW, Unwalla RJ, Singhaus RR Jr, Harris HA, Mewshaw RE. Estrogen receptor beta ligands: design and synthesis of new 2-phenyl-isoindole-1,3-diones. *Bioorg Med Chem Lett* 2007;17:118-122.
23. Umamatheswari S, Balaji B, Ramanathan M, Kabilan S. Synthesis, antimicrobial evaluation and QSAR studies of novel piperidin-4-yl-5-spiro-thiadiazoline derivatives. *Bioorg Med Chem Lett* 2010;20:6909-6914.
24. Hansch C, Verma RP. A QSAR study for the cytotoxic activities of taxoids against macrophage (MPhi)-like cells. *Eur J Med Chem* 2009;44:274-279.
25. Strike, version 1.8, Schrödinger, LLC, New York, NY, 2009.
26. Roy K. On some aspects of validation of predictive quantitative structure-activity relationship models. *Expert Opin Drug Discov* 2007;2:1567-1577.
27. LigPrep, version 2.3, Schrödinger, LLC, New York, NY, 2009.
28. Pike AC, Brzozowski AM, Hubbard RE, Bonn T, Thorsell AG, Engström O et al. Structure of the ligand-binding domain of oestrogen receptor beta in the presence of a partial agonist and a full antagonist. *Embo J* 1999;18:4608-4618.
29. Maestro, version 9.0, Schrödinger, LLC, New York, NY, 2009.
30. Prime, version 2.1, Schrödinger, LLC, New York, NY, 2009.
31. Glide, version 5.5, Schrödinger, LLC, New York, NY, 2009.
32. Pike AC. Lessons learnt from structural studies of the oestrogen receptor. *Best Pract Res Clin Endocrinol Metab* 2006;20:1-14.
33. Manas ES, Unwalla RJ, Xu ZB, Malamas MS, Miller CP, Harris HA et al. Structure-based design of estrogen receptor-beta selective ligands. *J Am Chem Soc* 2004;126:15106-15119.
34. Fang H, Tong W, Shi LM, Blair R, Perkins R, Branham W et al. Structure-activity relationships for a large diverse set of natural, synthetic, and environmental estrogens. *Chem Res Toxicol* 2001;14:280-294.
35. Chang HJ, Kim HJ, Chun HS. Quantitative structure-activity relationship (QSAR) for neuroprotective activity of terpenoids. *Life Sci* 2007;80:835-841.
36. Hansch C, Verma RP, Kurup A, Mekapati SB. The role of QSAR in dopamine interactions. *Bioorg Med Chem Lett* 2005;15:2149-2157.